Predictive Modeling and High-Pressure−High-Temperature Synthesis of Perovskites Containing Monovalent Silver

J.-H. Park,[†] P. M. Woodward,[‡] and J. B. Parise*[,†,§]

Center for High-Pressure Research, Department of Chemistry and Department of Geosciences, State University of New York, Stony Brook, New York 11790-2100, and Physics Department, Brookhaven National Laboratory, Upton, New York 11973

Received March 31, 1998. Revised Manuscript Received May 4, 1998

The program POTATO, which was developed to model distorted perovskite structures, has been used to assess the stability of hypothetical compositions and guide the synthesis of new materials at high pressures and high temperatures. The initial result of this effort is the synthesis of two new perovskites, $Ca_2NdAgTi_4O_{12}$ and $NdAgTi_2O_6$, which were synthesized at 14−14.5 GPa and 1000 °C using the uniaxial split sphere anvil type press (USSA-2000). Both compounds are perovskites distorted from the ideal cubic structure by octahedral tilting distortions. $Ca_2NdAgTi_4O_{12}$ contains a random distribution of $Ca^{2+}/Nd^{3+}/Ag^+$ ions on the A-site, whereas $NdAgTi_2O_6$ has a partially ordered distribution of Nd^{3+}/Ag^+ ions. $Ca_2NdAgTi_4O_{12}$ adopts the $GdFeO_3$ structure (Glazer tilt system $b^-a^+b^-$), space group *Pnma*, with $a = 5.44883(4)$, $b = 7.68915(6)$, and $c = 5.42290(3)$ Å. $NdAgTi_2O_6$ belongs to the tetragonal space group $P4/nbm$, with $a = 5.45337(3)$ and $c = 7.72934(6)$ Å. This structure can be derived from the simple cubic perovskite structure by rotations of the octahedra about the *c*-axis (Glazer tilt system $a^0a^0c^-$) and partial ordering of Nd^{3+} and Ag^+ ions into alternating layers, perpendicular to the *c*-axis.

Introduction

The perovskite structure type is one of the most frequently encountered in all of solid-state inorganic chemistry. The ideal perovskite structure, stoichiometry AMX_3, is composed of a three-dimensional framework of corner-linked MX_6 octahedra. The structure is completed by filling the large cavities in the MX_3 network with A cations, which are surrounded by 12 equidistant anions. Although there are many compounds that adopt the ideal cubic structure, distortions from the ideal structure are commonplace.[1] Distortion mechanisms include octahedral tilting,[2−4] cation displacements,[5−7] Jahn−Teller distortions of the octahedra[8,9] and, in $AA'MM'X_6$ perovskites, cation ordering.[10−12]

Recently, the program POTATO was developed to model octahedral tilting distortions in perovskites.[13] This program generates idealized perovskite structures based on the size of the octahedra (which can be accurately estimated from ionic radii or bond valence concepts), the octahedral tilt system, and the magnitude of the tilt angles. One potential use of POTATO is as a predictive tool to evaluate the stability of hypothetical perovskite compositions. In this role, POTATO can be used to select combinations of ions that have ionic radii and bonding preferences complimentary to each other, thereby increasing the probability that synthetic attempts will lead to new materials.

High-pressure−high-temperature (HPHT) synthetic routes are an effective way of synthesizing novel metal oxide compounds.[14] Furthermore, the high packing density of the perovskite structure makes HPHT methods particularly well suited to synthesis of new perovskites that can then be retained at ambient conditions by quenching the temperature and slowly releasing pressure. The combination of POTATO modeling to predict compositions stabilized in the perovskite structure and HPHT synthesis of these compounds represents an advanced approach to searching for new perovskites. Using this method for the first time, we report the synthesis and structural characterization of two new silver-containing perovskite compounds, $NdAgTi_2O_6$ and $NdAgCa_2Ti_4O_{12}$. It's utility in this role could prove to be particularly important in high-pres-

* Author to whom correspondence should be sent.
[†] Center for High-Pressure Research, Department of Chemistry.
[‡] Physics Department.
[§] Center for High-Pressure Research, Department of Geosciences.

(1) Woodward, P. M. *Acta Crystallogr.* **1997**, *B53*, 44.
(2) Glazer, A. M. *Acta Crystallogr.* **1972**, *B28*, 3384.
(3) Burns, G.; Glazer, A. M. *Space Groups for Solid State Scientists*, 2nd edition; Academic: Boston, 1990; Appendix A9−6.
(4) Woodward, P. M. *Acta Crystallogr.* **1997**, *B53*, 32.
(5) Megaw, H. D.; Darlington, C. N. W. *Acta Crystallogr.* **1975**, *A31*, 161.
(6) Thomas, N. W.; Beitollahi, A. *Acta Crystallogr.* **1994**, *B50*, 549.
(7) Cereceda, N.; Noheda, B.; Iglesias, T.; Fernandez-del-Castillo, J. R.; Gonzalo, J. A.; Duan, N.; Wang, Y. L.; Cox, D. E.; Shirane, G. *Phys. Rev.* **1997**, *B55*, 6174.
(8) Okazaki, A.; Y. Suemune, *J. Phys. Soc. Jpn.* **1961**, *16*, 176.
(9) Reinen, C.; Weitzel, H. *Z. Anorg. Allg. Chem.* **1976**, *424*, 31.
(10) Anderson, M. T.; Greenwood, K. B.; Taylor, G. A.; Poeppelmeier, K. R. *Prog. Solid State Chem.* **1993**, *22*, 197.
(11) Setter, N.; Cross, L. E. *J. Mater. Sci.* **1980**, *15*, 2478.
(12) Woodward, P. M. Ph.D. Thesis, Oregon State University, Ch. 4−6, 1996.
(13) Woodward, P. M. *J. Appl. Crystallogr.* **1997**, *30*, 206.
(14) Park, J.-H.; Parise, J. B. *Chem. Mater.* **1995**, *7*, 1055.

10.1021/cm980212j CCC: $15.00
Published on Web 07/31/1998

sure synthesis applications where access to time on a high-pressure synthetic apparatus is a limiting factor.

Cation Ordering

Double substitution on the octahedral site leads to cation ordering when the ionic attributes (ionic radius, formal charge, covalent bonding interactions) of the *M* and *M*' cations are sufficiently different.[10−12,15] For a 1:1 ratio of M and M', the most stable ordering configuration is invariably a rock salt arrangement. A rare exception to this rule is La_2CuSnO_6, where the Cu^{2+} and Sn^{4+} cations order in layers.[16] This unusual ordered arrangement of octahedral cations appears to be stabilized by the Jahn−Teller distortions about Cu^{2+} and a very delicate balance of ionic interactions.[10]

In contrast to ordering of M/M' cations, there are relatively few examples of A-cation ordering. Examples of A-cation ordering can generally be divided into two categories: those driven by charge and/or size differences between A and A' cations and those driven by differences in the coordination preferences of A and A'. Examples of the former type of ordering include $La_{0.33}\square_{0.67}NbO_3$,[17] $La_{0.67}\square_{0.33}NbO_3$,[18] $La_{0.67-x}Li_{3x}\square_{0.33-2x}TiO_3$,[19] $Na_{0.5+x}La_{0.5-3x}Th_{2x}TiO_3$,[20] $Na_{0.67}Th_{0.33}TiO_3$,[21] $La_{1.33}\square_{0.67}MgWO_6$,[22] $NaLaMgWO_6$,[23] and $Pb_{0.5}Ca_{0.5}TiO_3$.[24] With the exception of $Pb_{0.5}Ca_{0.5}TiO_3$, all of the aforementioned compounds show layered A-cation ordering, rather than the rock salt arrangement associated with M/M' ordering. It should also be noted that $La_{1.33}\square_{0.67}MgWO_6$ and $NaLaMgWO_6$ contain rock salt ordering of the M/M' cations in addition to layered A-cation ordering. Interestingly, $NaLaTi_2O_6$, although it has the same A cations as $NaLaMgWO_6$, does not show long range ordering of Na^+ and La^{3+}.[25]

Examples of the second type of A-cation ordering, those arising from differences in the coordination preferences of A and A', belong almost exclusively to a family of compounds with stoichiometry $A'A_3M_4O_{12}$ ($A = Cu^{2+}$, Mn^{2+}; A' = Na, Ca, Y, Nd, La, Th; M = Mn, Ti, Ge, Ru). Members of this family include $NaCu_3Mn_4O_{12}$,[26] $CaCu_3Ti_4O_{12}$,[27] $CaCu_3Ge_4O_{12}$,[28] $NdCu_3Ru_4O_{12}$,[29] and the parent compound of this structure type, $NaMn_3Mn_4O_{12}$.[30] All of these compounds are perovskites distorted from the ideal structure by an octahedral tilting arrangement described by the Glazer tilt system[31] $a^+a^+a^+$.[2−4] The distortion of the oxygen network in this tilt system is such that 25% of the A-site cations have a distorted cubooctahedral coordination with 12 equidistant oxygen neighbors, whereas the remaining 75% have square-planar coordination,[1] as shown in Table 1. Thus it becomes apparent why this tilt system is adopted by $ACu^{2+}{}_3M_4O_{12}$ compounds. The smaller, Jahn−Teller Cu^{2+} cations can fully occupy the square-planar sites, whereas the larger A cations can occupy the cubooctahedral sites. The $a^+a^+a^+$ tilt system is not the only tilt system where octahedral tilting and A-cation coordination preferences can act in concert to stabilize coordination-driven A-cation ordering. Octahedral tilting distortions in the tilt systems $a^+a^+c^-$, $a^0b^+b^+$, and $a^0b^+b^-$ also lead to a distribution of A-cation sites with contrasting coordination spheres (see Table 1). However, excluding members of the $a^+a^+a^+$ tilt system, only one example of coordination driven A-site cation ordering is known, $CaFeTi_2O_6$ ($a^+a^+c^-$).[32]

To maximize the driving force for A-cation ordering, one needs to maximize the differences in charge, size and/or coordination preferences between the various cations on the A-site. From this perspective the Ag^+ ion is an attractive candidate to be used in combination with other ions. The ionic radius of Ag^+ (1.28 Å)[33] is considerably larger than the radii of the trivalent cations in the lanthanide series (0.977−1.16 Å),[34] so that A-site-cation ordering might be expected in $AgLn^{3+}M^{4+}{}_2O_6$ compositions. Furthermore, unlike the alkali, alkaline-earth, and lanthanide cations, Ag^+ occasionally adopts square planar coordination (i.e., Ag_2AsO_4[35] and $Ag_{1.8}Mn_8O_{16}$[36]), which raises the possibility that it might also be used in coordination-driven A-cation ordering compositions. Despite its apparent compatibility with the perovskite, structure there are only two known perovskites that contain Ag^+, $AgNbO_3$, and $AgTaO_3$.[37] The reason for this scarcity of silver-containing perovskites stems not from crystal chemistry arguments, but rather from the low thermal stability of silver oxides.[38] This low stability severely limits the reaction temperatures that can be used, and consequently conventional

(15) Wells, A. F. *Structural Inorganic Chemistry*, 5th ed.; Clarendon: Oxford, 1984.
(16) Anderson, M. T.; Poeppelmeier, K. R. *Chem. Mater.* **1991**, *3*, 476.
(17) Iyer, P. N.; Smith, A. J. *Acta Crystallogr.* **1967**, *23*, 740.
(18) Abe, M.; Uchino, K. *Mater. Res. Bull.* **1974**, *9*, 147.
(19) Forquet, J. L.; Duroy, H.; Crosnier-Lopez, M. P. *J. Solid State Chem.* **1996**, *127*, 283.
(20) Mitchell, R. H.; Chakhmouradian, A. R. *J. Solid State Chem.*, in press.
(21) Zhu, W. J.; Hor, P. H. *J. Solid State Chem.* **1995**, *120*, 208.
(22) Torii, Y. *Chem. Lett.* **1979**, *1979*, 1215.
(23) Sekiya, T.; Yamamoto, T.; Torii, Y. *Bull. Chem. Soc. Jpn.* **1984**, *57*, 1859.
(24) King, G.; Goo, E.; Yamamoto, T.; Okazaki, K. *J. Am. Ceram. Soc.* **1988**, *71*, 454.
(25) Agranovskaya, A. I. *Bull. Acad. Sci. USSR Phys. Ser.* **1960**, *24*, 1271.
(26) Chenevas, J.; Joubert, J. C.; Marezio, M.; Bochu, B. *J. Solid State Chem.* **1975**, *14*, 25.
(27) Bochu, B.; Deschizeaux, N. N.; Joubert, J. C.; Collomb, A.; Chenevas, J.; Marezio, M. *J. Solid State Chem.* **1979**, *29*, 291.
(28) Ozaki, Y.; Ghedira, M.; Chenevas, J.; Joubert, J. C.; Marezio, M. *Acta Crystallogr.* **1977**, *B33*, 3615.
(29) Müller, J.; Haouzi, A.; Laviron, C.; Labeau M.; Joubert, J. C. *Mater. Res. Bull.* **1986**, *21*, 1131.
(30) Marezio, M.; Dernier, P. D.; Chenevas, J.; Joubert, J. C. *J. Solid State Chem.* **1973**, *6*, 16.
(31) Glazer provided a notation system for describing octahedral tilting distortions in perovskites by specifying the magnitude and phase of the octahedral rotations about each of the Cartesian axes. The letters in Glazer notation reflect the magnitude of the rotation about a given axis with respect to the rotations about the other axes (i.e., if the rotations about all three axes are equivalent and in phase then the tilt system is $a^+a^+a^+$, whereas if the rotations about a and b are equivalent but different in magnitude from the rotation about c then the tilt system becomes $a^+a^+c^+$). The superscripts denote whether the octahedra in neighboring layers, perpendicular to the rotation axis, are rotated the same direction (+), in opposite directions (−) or not rotated at all (0). If all rotations about a given axis are in the same direction (+), this is often called in phase tilting, whereas out-of-phase tilting refers to the case where the rotation direction alternates from one layer to the next (−). For a more detailed description please see the refs 2, 3, 4, and Glazer, A. M. *Acta Crystallogr.* **1975**, *A31*, 756.
(32) Leinenweber, K.; Parise, J. B. *J. Solid State Chem.* **1995**, *114*, 277.
(33) Unless otherwise mentioned, eight-coordinate radii will be used for the A-site cations.
(34) Shannon, R. D. *Acta Crystallogr.* **1976**, *A32*, 751.
(35) Helmholz, L.; Levine, R. *J. Am. Chem. Soc.* **1942**, *64*, 354.
(36) Chang, F. M.; Jansen, M. *Angew. Chem.* **1984**, *96*, 902.
(37) Francombe, M. H.; Lewis, B. *Acta Crystallogr.* **1958**, *11*, 175.
(38) *CRC Handbook of Chemistry and Physics*, 77th ed.; Ride, D. R. Ed.; CRC: Boca Raton, FL 1996−1997.

Table 1. A−O Bond Distances in Tilt Systems with Potential for Coordination-Driven A-Cation Ordering

tilt system	bond angles (°)[a]	unit cell volume (Å^3)	Wyckoff position	geometry	A−O bond distances (Å)[b]
$a^+a^+a^+$	13.3	409.2	2a	dist. cubo-octahedron	**12 × 2.63**
			6b	square planar	**4 × 2.00**
					4 × 2.77
					4 × 3.25
$a^+a^+c^-$	11.3, 15.9	412.1	2b	square planar	**4 × 2.00**
					4 × 3.02
					4 × 3.14
			2a	dist. tetrahedral	**4 × 2.08**
					4 × 2.67
					4 × 3.21
			4d	dist. tetrahedral	**4 × 2.25**
					4 × 2.67
					2 × 2.69
					2 × 3.39
$a^0b^+b^+$	14.5	423.3	2a	square planar	**4 × 2.00**
					8 × 3.04
			2b	square prismatic	**8 × 2.38**
					4 × 3.37
			4c	rectangular planar	**4 × 2.28**
					4 × 2.77
					4 × 2.96
$a^0b^-b^+$	16.4	408.0	4c	dist. tetrahedral	**4 × 2.00**
					2 × 2.76
					4 × 3.01
					2 × 3.22
			4c	dist. trigonal prismatic	**4 × 2.26**
					2 × 2.47
					2 × 2.71
					2 × 2.84
					2 × 3.43

[a] All structures were calculated with POTATO, using an M−O bond distance of 1.96 Å and the criteria that the smallest A-cation site should have four 2.00 Å bonds for its first coordination sphere. [b] A−O distances that make up the first coordination sphere are shown in bold.

solid-state synthesis routes are not generally suitable. Recently developed ion-exchange and HPHT techniques however, have been used to synthesize many new silver-containing compounds. The former has been applied to parent materials such as alkali Ruddledsen−Popper family of titanates and niobates, using molten $AgNO_3$ to obtain perovskite-related compounds with silver layers.[39−41] The latter has been used to place Ag^{3+} in a $LaCuO_3$ lattice.[42] Because the stoichiometric perovskite framework is not conducive to ion exchange, HPHT techniques represent the most promising route to stabilizing new perovskites containing Ag^+.

POTATO Modeling

The first step in our quest to synthesize A-cation ordered perovskites containing Ag^+ was to use POTATO to generate hypothetical perovskite crystal structures. The M−O distances, which determine the size of the octahedra, were selected to optimize the bond valence[43,44] of the M cation. The tilt angles were then varied to optimize the valences of the A-site cations. All bond valence and Madelung energy calculations were performed with the program Eutax.[45] Finally, synthetic attempts were then undertaken for the most promising compositions.

In selecting compositions we chose to search for combinations of ions that would form perovskites belonging to the $a^0b^+b^+$ tilt system. This decision was based on the fact that no representatives of this tilt system are known. Thus, successful formation of an $a^0b^+b^+$ compound would be a dramatic representation of the power of the POTATO/HPHT approach. The $a^0b^+b^+$ distortion produces a structure belonging to space group *I*4/*mmm*, with three distinct crystallographic sites for the A cations, as shown in Table 1. Like the $a^+a^+a^+$ tilt system, some of the A cation sites are better suited for larger A cations (2*b* and 4*c* sites), whereas the remainder of the sites have shorter A−O bond distances and a square planar coordination (2*a*). However, the size difference between the 'large' and 'small' A-cation sites in $a^0b^+b^+$ is much smaller than that in $a^+a^+a^+$, which makes it more difficult to find suitable combinations of A cations. As a consequence, one must find either large square planar ions or small eight-coordinate ions. (This is also true of the $a^+a^+c^-$ and $a^0b^-b^+$ tilt systems, which helps to explain the scarcity of perovskites in these tilt systems.) Consulting Shannon's ionic radii, one finds that, with the exception of the ions of silver, all square planar ions have radii in the range 0.49−0.68 Å.[34] In contrast, the ionic radius of Ag^+ in square planar coordination is 1.02 Å. Therefore, the only suitable 'large' square planar ion would seem to be Ag^+. If on the other hand one opts to look

(39) Toda, K.; Kurita, S.; Sato, M. *Solid State Ionics* **1995**, *81*, 267.
(40) Sato, M. M.; Toda, K.; Watanabe, J.; Uematsu, K. *Nippon Kagaku Kaishi* **1993**, *1993*, 640.
(41) Sato, M.; Watanabe, J.; Uematsu, K. *J. Solid State Chem.* **1993**, *107*, 460.
(42) Webb, A. W.; Skelton, E. F.; Quadri, S. B.; Carpenter, J. E. R. *J. Solid State Chem.* **1993**, *102*, 519.
(43) Brown, I. D. *Structure and Bonding in Crystals*; O'Keeffe, M.; Navrotsky, A., Eds., Academic: New York: 1981; Vol. 2, pp 1−30.
(44) O'Keeffe, M. *Struct. Bonding (Berlin)* **1989**, *71*, 162.
(45) O'Keeffe, M. *Eutax*, EMLab Software, Phoenix, AZ.

Table 2. Results of POTATO Modeling Calculations

compound	tilt system	tilt angles (°)	lattice energy (kJ/mol)	volume (Å^3)	bond valences A1	A2	A3	M[e]
$NdCa_2AgTi_4O_{12}$	$a^0b^+b^+$[a]	0,7	−71,099	467.7	2.52	1.56	1.16	4.06
	$b^-a^+b^-$[b]	−6.8,6.8	−70,784	462.0	2.69	1.80	1.16	4.06
$NdSr_2AgTi_4O_{12}$	$a^0b^+b^+$	0,7	−71,099	467.7	2.52	2.35	1.16	4.06
	$b^-a^+b^-$	−6.8,6.8	−70,784	462.0	2.69	2.70	1.16	4.06
$LaSr_2AgRu_4O_{12}$	$a^0b^+b^+$	0,7.9	−70,482	478.2	2.86	2.26	1.16	4.04
	$b^-a^+b^-$	−8.4,8.4	−70,396	465.7	3.37	2.91	1.16	4.04
	$b^-a^+b^-$[c]	−6.0,6.0	−69,396	480.7	2.73	2.36	1.01	4.04
$MgZn_2CuTi_4O_{12}$	$a^0b^+b^+$	0,15.5	−72,069	415.4	1.34	1.31	1.97	4.06
$CaCa_2CuTi_4O_{12}$	$a^0b^+b^+$	0,15.5	−72,069	415.4	2.82	2.66	1.97	4.06
$Ca_2FeFeTi_4O_{12}$								
model structure	$a^+a^+c^-$[d]	11.3,16.5	−71,195	409.5	2.83	2.35	1.83	4.04
actual structure	$a^+a^+c^-$		−71,852	426.7	2.26	1.78	1.70	4.05

[a] For the $a^0b^+b^+$ tilt system, the A1 cation has 8-fold coordination (Nd, La, Mg, Ca), the A2 cation 4+4 distorted tetrahedral coordination (Ca, Sr, Zn), and the A3 cation square planar coordination (Ag, Cu). [b] In tilt system $b^-a^+b^-$, A1, A2, and A3 occupy the same crystallographic site and, although permitted by symmetry, this ion has not been shifted off of its ideal site. [c] With the silver bond valence at 1.16, all of the A-cations are overbonded; therefore, the tilting has been relaxed to optimize the bond valences. [d] For $CaFeTi_2O_6$, A1 is calcium, A2 is tetrahedral iron, and A3 is square planar iron. [e] The M cations are either Ti^{4+} or Ru^{4+}: in all model calculations, the Ti—O distance is taken to be 1.96 Å and the Ru—O distance 1.98 Å.

for a small eight-coordinate ion, the choice of square planar ion is less critical, due to the rather narrow distribution of radii among the remaining square planar ions. The most obvious choice is Cu^{2+} (0.57 Å), because of its strong preference for square planar coordination. There is also considerable flexibility in the choice of the M cation, but here we choose to concentrate on two tetravalent cations that are commonly found in perovskites, Ti^{4+} and Ru^{4+}.

Based on the arguments just made, we looked for combinations of ions that would form stable $a^0b^+b^+$ compounds with either Ag^+ or Cu^{2+} on the square planar (2a) site. Table 2 summarizes the results of these calculations. Defining the structure that optimizes the bond valences of all of its constituent ions is somewhat arbitrary. We chose for sake of comparison to maintain the bond valences of Ag^+ and Cu^{2+} at values of 1.16 and 1.97 for all compositions. When tilt angles become large, the $b^-a^+b^-$ tilt system is generally the most stable configuration, therefore optimized structures in that tilt system were also calculated for the Ag^+-containing compositions. This was not done for the Cu^{2+}-containing compositions because the small size and strong preference for square planar coordination make it unlikely that Cu^{2+} would be stable on the A-site of an $b^-a^+b^-$ perovskite.

Beginning with $Ca_2NdAgTi_4O_{12}$ we see that the smaller Nd^{3+} (1.109 Å) and Ca^{2+} (1.12 Å) ions are underbonded in the $a^0b^+b^+$ tilt system. The bond valences of both cations are closer to their formal oxidation state values in the idealized $b^-a^+b^-$ structure. Therefore, the bond valence sums suggest that $Ca_2NdAgTi_4O_{12}$ should form a stable $b^-a^+b^-$ perovskite. Another important feature illustrated by these calculations, is that for a constant Ag^+ bond valence the $b^-a^+b^-$ structure has a smaller unit cell volume. In fact among the tilt systems listed in Table 1, the $a^0b^+b^+$ tilt system has the largest unit cell volume (least dense framework). A potential consequence of this is that, all other things being equal, high-pressure synthesis routes should favor those tilt systems which have the highest packing densities.

One of the obstacles to formation of a $a^0b^+b^+$ perovskite from $Ca_2NdAgTi_4O_{12}$ is that the Ca^{2+} ion is too small for the $AgTi_4O_{12}^{7-}$ framework. A potential solution to this problem is to replace it with the larger Sr^{2+} ion (1.26 Å). This results in Sr^{2+} being moderately overbonded in the $a^0b^+b^+$ structure, but much too large for the $b^-a^+b^-$ structure. Therefore, although the A-cation bond valences predicted for $Sr_2NdAgTi_4O_{12}$ are less than ideal for formation of a single-phase perovskite, substitution of Sr^{2+} for Ca^{2+} may help to stabilize the $a^0b^+b^+$ tilt system over the $b^-a^+b^-$ tilt system. Also keep in mind that octahedral distortions can occur to accommodate oversized and/or undersized cations. These distortions can make the bond valences more reasonable than predicted in the model structure, as illustrated by the bond valences of $CaFeTi_2O_6$ in Table 2.

The final Ag^+-containing target composition was $Sr_2LaAgRu_4O_{12}$. Table 2 shows that model structures generated using this composition have very reasonable bond valences in both the $a^0b^+b^+$ and $b^-a^+b^-$ tilt systems. Due to the qualitative nature of the modeling it is difficult to predict which configuration will be the most stable. However, $Sr_2LaAgRu_4O_{12}$ would certainly appear to be a promising candidate to form the first $a^0b^+b^+$ perovskite. On the other hand, the prospects for forming a stable $a^0b^+b^+$ perovskite with Cu^{2+} on the square planar site do not look good. Ca^{2+} is much too large for the $CuTi_4O_{12}^{6-}$ framework, but the next largest divalent ions, such as Mg^{2+} and Zn^{2+}, are far too small. Thus, we chose to limit our synthetic attempts to the Ag^+-containing compositions.

In summary, the POTATO modeling predicts that the $b^-a^+b^-$ tilt system will be the most stable configuration for $Ca_2NdAgTi_4O_{12}$, whereas $NdSr_2AgTi_4O_{12}$ if it forms a single-phase perovskite should favor the $a^0b^+b^+$ tilt system over $b^-a^+b^-$, and $LaSr_2AgRu_4O_{12}$ appears capable of forming stable structures in either tilt system. No divalent ions can be found which, in combination with Cu^{2+} on the square planar site, appear likely to form an $a^0b^+b^+$ perovskite. Finally, it should be clearly stated that our modeling approach says nothing about the stability of competing phases, such as $SrTiO_3$, $CaTiO_3$, and $SrRuO_3$.

Experimental Section

All HPHT synthetic attempts were carried out at 14−14.5 GPa and 1000 °C for 3 h, followed by temperature quenching

and slow decompression using the 2000-ton Uniaxial Split Sphere high-pressure apparatus (USSA 2000) at Stony Brook. Details of the cell assembly along with the temperature and the pressure calibration have been reported elsewhere.[46,47] Our first target composition, $Ca_2NdAgTi_4O_{12}$, was prepared from a stoichiometric mixture of reagent grade $CaTiO_3$, Nd_2O_3, Ag_2O, and TiO_2. The reagents were thoroughly ground and sealed in an Au capsule with an inside diameter of 3.2 mm and a wall thickness of 0.1 mm. Following the HPHT run, conventional powder XRD, using a SCINTAG diffractometer with $\theta-\theta$ geometry and CuKα radiation, showed the sample to be almost exclusively a perovskite. However, a small amount of Srilankite,[48] a high-pressure polymorph of TiO_2, was also present.[49] Electron probe microanalysis showed that the sample is homogeneous and possess a metal ratio consistent with the desired product, $NdCa_2AgTi_4O_{12}$.

The same experimental procedures were then repeated with $SrTiO_3$ in place of $CaTiO_3$, with the intention of finding the analogous compound, $Sr_2NdAgTi_4O_{12}$. The results of the XRD and electron microprobe analysis showed the sample to be a mixture of at least three phases. One phase was clearly $SrTiO_3$ and the other phases belonged to the solid solution $Sr_{1-2x}Nd_xAg_xTiO_3$. This result suggested the existence of $NdAgTi_2O_6$ and prompted us to repeat the aforementioned experimental procedures starting from Nd_2O_3, Ag_2O, and TiO_2. Conventional powder XRD patterns indicated the product of this run to be a single-phase perovskite, with metal ratios determined using electron probe microanalysis to be 0.97(2)-Nd:1.00(2)Ag:1.97(1)Ti. Once again a small amount of Srilankite was present as an impurity phase.[49] Synthesis of $Sr_2LaAgRu_4O_{12}$ from $SrRuO_3$, RuO_2, Ag_2O, and La_2O_3 was not successful. The XRD analysis showed that the HPHT treatment reduced Ag_2O to silver metal, but the remaining starting materials did not appear to react.

Synchrotron powder XRD data were collected at the X7A beamline at the National Synchrotron Light Source, Brookhaven National Laboratory. Samples were first loaded into 0.2-mm diameter glass capillaries, which were freely rotated at 1−2 Hz during data collection to avoid potential problems with preferred orientation or texture. Monochromatic radiation was obtained using a channel-cut Ge (111) monochromator. The data were collected by step scanning over the approximate angular range $10° < 2\theta < 60°$ in increments of 0.25° using a position sensitive detector (PSD).[50−52] Rietveld refinements[53] were carried out using the GSAS software suite.[54]

Results

Rietveld refinements confirm that $Ca_2NdAgTi_4O_{12}$ is a perovskite. The structure has *Pnma* symmetry, as expected for a member of the $a^-b^+a^-$ tilt system, with $a = 5.44883(4)$, $b = 7.68915(6)$, and $c = 5.42290(3)$ Å. The refinement parameters are summarized in Tables 3 and 4, select bond distances and angles are given in Table 5, and cation bond valences are listed in Table 6. The observed, calculated and difference patterns from the Rietveld refinement are shown in Figure 1, and a representation of the structure is illustrated in Figure 2. Even though the Ca^{2+}, Nd^{3+}, and Ag^+ ions are randomly distributed on the A-site, the thermal parameters of all ions are reasonable. The observed bond valences are very close to those predicted by POTATO. Based on the fractional coordinates of the oxygen ions the octahedral tilt angles are estimated to be 7.4(1)° (clockwise) for the out of phase tilts about the *x* and *z* axes (b^-) and −7.7(2)° (counterclockwise) for the in phase tilt about the *y* axis (a^+).[55] These values are slightly larger than predicted in the modeling section, presumably because once the A cation shifts off of the 0,1/4,0 position it relieves the electron−electron repulsion associated with short A−O bonds and allows the TiO_3 framework to collapse further.[1]

Table 3. Crystallographic Data for $NdAgTi_2O_6$ and $Ca_2NdAgTi_4O_{12}$

data	$NdAgTi_2O_6$	$Ca_2NdAgTi_4O_{12}$
wavelength (Å)	0.650653	0.79990
2θ range (°)	3−60	9−90
space group	*P*4/*nbm*	*Pnma*
cell parameters (Å)	$a = 5.45337(3)$	$a = 5.44883(4)$
	$c = 7.72934(6)$	$b = 7.68915(6)$
		$c = 5.42290(3)$
no. of variables	17	16
no. of data	512	728
R_{wp}	0.0673	0.0620
R_p	0.0439	0.0412
$R(F^2)$	0.0483	0.0816
reduced χ^2	17.49	12.67

All peaks in the $NdAgTi_2O_6$ diffraction pattern could be indexed to either a tetragonal perovskite, with a $\sqrt{2}a_p \times \sqrt{2}a_p \times 2a_p$ unit cell (a_p = the simple cubic perovskite cell dimension) or Srilankite. The extinction conditions for $NdAgTi_2O_6$ are consistent with the tetragonal space group *P*4/*nbm* (No. 125). The presence of the (001) reflection at 4.84° 2θ indicates that layered cation ordering, perpendicular to the *c* axis, has occurred.[10,23] This type of ordering by itself results in a doubling of the *c* axis and a reduction in symmetry from *Pm*3*m* to *P*4/*mmm*.[19,20] The enlarged unit cell and *P*4/*nbm* symmetry suggest that more than one type of symmetry-lowering distortion mechanism is at work in $NdAgTi_2O_6$. In analyzing the situation we first noted that *P*4/*nbm* is an isomorphic subgroup of *I*4/*mcm*, which is the expected space group for a compound that has undergone $a^0a^0c^-$ octahedral tilting.[2−4] A subsequent symmetry analysis showed that the combination of layered A-cation ordering and an $a^0a^0c^-$ octahedral tilting distortion results in a structure with *P*4/*nbm* symmetry. Rietveld refinements confirm the presence of both distortion mechanisms. The octahedral tilting angle about the *c* axis is estimated to be 7.95(1)°.

The degree of Nd^{3+}/Ag^+ ordering was estimated by refining the fractional parameter for each A-site so that both A-sites remain fully occupied and an Ag:Nd ratio

(46) Park, J.-H.; Parise, J. B. *Mater. Res. Bull.* **1997**, *32*, 1617.
(47) Liebermann, R. C.; Wang, Y. *High-Pressure Research: Application to Earth and Planery Sciences*; Terrapub: Tokyo, 1992.
(48) Willgallis, A.; Hantl, H. *Z. Kristallogr.* **1983**, *164*, 59.
(49) The presence of Srilankite is a consequence of a small amount of silver volatilizing onto the Au capsule during the HPHT treatment. As a result of this loss of titanium and silver, one would expect the Nd:Ag and Nd:Ag:Ca ratios to deviate slightly from their stoichiometric values. The accuracy of the SEM elemental analysis is not sufficient to quantitatively measure such a small deviation from stoichiometry. However, when the A-site occupancy is varied in the Rietveld refinements (see Table 4), the average electron density on the A-site refines very close to the value expected for a perfectly stoichiometric compound. Thus, both $NdAgTi_2O_6$ and $Ca_2NdAgTi_4O_{12}$ appear to be nearly stoichiometric within experimental accuracy. The explanation for the apparent loss of neodymium and calcium (necessary to achieve a mass balance between starting and final products) is not clear. One possibility is that a small amount of undetected amorphous product is also present.
(50) Smith, G. C. *Synth. Rad. News* **1991**, *4*, 24.
(51) Cox, D. E.; Toby, B. H.; Eddy, M. M. *Aust. J. Phys.* **1988**, *41*, 117.
(52) Cox, D. E. In *Synchrotron Radiation Crystallography*; Coppens, P.; Ed.; Academic: London, 1992.
(53) Rietveld, H. M. *J. Appl. Crystallogr.* **1969**, *2*, 65.
(54) Larson, A. C.; von Dreele, R. B. *General Structure Analysis System*; Los Alamos National Laboratory: Los Alamos, NM, 1994.
(55) Woodward, P. M.; Vogt, T.; Cox, D. E.; Arulraj, A.; Rao, C. N. R.; Karen, P.; Cheetham, A. K. Submitted to *Chem. Mater.*

Table 4. Atomic Positional Parameters, Equivalent Isotropic Displacement Coeffiecnts (Å² × 10³), and Anisotropic Displacement Parameters of Metal Ions

$NdAgTi_2O_6$	*x*	*y*	*z*	occupancy	U_{iso}
Nd(1)	0.75000	0.25000	0.00000	0.75(2)	0.0120(1)
Nd(2)	0.75000	0.25000	0.50000	0.25(2)	0.0120(1)
Ag(1)	0.75000	0.25000	0.50000	0.75(2)	0.0120(1)
Ag(2)	0.75000	0.25000	0.00000	0.25(2)	0.0120(1)
Ti	0.25000	0.25000	0.2492(8)	1.00000	0.0058(5)
O(1)	0.25000	0.25000	0.00000	1.00000	0.059(3)
O(2)	0.25000	0.25000	0.50000	1.00000	0.059(3)
O(3)	0.4651(5)	0.9651(5)	0.233(1)	1.00000	0.008(1)

	U_{11}	U_{22}	U_{33}	U_{12}	U_{13}	U_{23}
Ag/Nd	0.0128(1)	0.0128(1)	0.0104(3)	0.0	0.0	0.0
Ti	0.0087(4)	0.0087(4)	−0.00023(7)	0.0	0.0	0.0

$Ca_2NdAgTi_4O_{12}$	*x*	*y*	*z*	occupancy	U_{iso}
Ca	0.0190(1)	0.25000	−0.0044(3)	0.503(1)	0.00564(9)
Nd	0.0190(1)	0.25000	−0.0044(3)	0.253(1)	0.00564(9)
Ag	0.0190(1)	0.25000	−0.0044(3)	0.253(1)	0.00564(9)
Ti	0.50000	0.00000	0.00000	1.00000	0.0033(2)
O(1)	0.7180(7)	−0.0323(6)	0.2854(7)	1.00000	0.0042(9)
O(2)	−0.0146(9)	0.25000	0.434(1)	1.00000	0.009(2)

Table 5. Select Interatomic Distances (Å) and Angles (°)

$NdAgTi_2O_6$	distance	angle	degree
Ti—O(4)	1.930(7)	O(4)—Ti—O(5)	180.0
Ti—O(5)	1.934(7)	O(4)—Ti—O(6) × 4	86.3(3)
Ti—O(6) × 4	1.9510(8)	O(5)—Ti—O(6) × 4	93.7(3)
Nd(1)—O(4) × 4[a]	2.727(2)	O(6)—Ti—O(6) × 4	89.75(4)
Nd(1)—O(6) × 4[a]	2.842(7)	O(6)—Ti—O(6) × 2	172.0(5)
Nd(1)—O(6) × 4[a]	2.450(7)	Ti—O(4)—Ti	180.0
Ag(1)—O(5) × 4[b]	2.727(2)	Ti—O(5)—Ti	180.0
Ag(1)—O(6) × 4[b]	2.646(8)	Ti—O(6)—Ti	162.0(3)
Ag(1)—O(6) × 4[b]	3.013(7)		
$Ca_2NdAgTi_4O_{12}$	distance	angle	degree
Ti—O(5) × 2	1.944(4)	O(5)—Ti—O(5) × 2	180.0
Ti—O(5) × 2	1.967(4)	O(5)—Ti—O(5) × 2	89.43(4)
Ti—O(6) × 2	1.957(1)	O(5)—Ti—O(5) × 2	90.57(4)
Ca(1)—O(5) × 2[c]	3.142(3)	O(5)—Ti—O(6) × 2	89.1 (2)
Ca(1)—O(5) × 2[c]	2.402(3)	O(5)—Ti—O(6) × 2	90.9(2)
Ca(1)—O(5) × 2[c]	2.679(5)	O(5)—Ti—O(6) × 2	89.7(2)
Ca(1)—O(5) × 2[c]	2.702(5)	O(5)—Ti—O(6) × 2	90.3(2)
Ca(1)—O(6)[c]	3.051(6)	O(6)—Ti—O(6)	180.0
Ca(1)—O(6)[c]	2.384(6)	Ti—O(5)—Ti	158.8(2)
Ca(1)—O(6)[c]	2.932(5)	Ti—O(6)—Ti	158.4(3)
Ca(1)—O(6)[c]	2.570(5)		

[a] Nd(1) represents the Nd-dominated site. [b] Ag(1) represents the Ag-dominated site. [c] Ca(1) represents the Cd/Nd/Ag disordered site.

Table 6. Cation Bond Valences

cation	$NdAgTi_2O_6$	$Ca_2NdAgTi_4O_{12}$
Ag	0.90	1.16
Nd	2.96	2.69
Ca	—	1.91
Ti	4.23	4.06

of unity is maintained. The refinement shows that 75% of the Nd^{3+} is accommodated on the 2c site, whereas a corresponding amount of Ag^+ resides on the 2d site. Bond valence calculations support this conclusion. The temperature factors of these sites were varied but constrained to be equal, to avoid correlation between the thermal parameters and fractional occupancies. The refinement parameters are summarized in Tables 3 and 4, and the observed, calculated, and difference patterns are shown in Figure 3. A representation of the structure is shown in Figure 4. The supercell peaks that arise due to cation ordering (those violating the body centered reflection conditions) were observed to be broader than the subcell peaks, indicating the presence of antiphase domains in the Ag—Nd—Ag—Nd stacking sequence.[56] To estimate the concentration of antiphase boundaries a Williamson—Hall type analysis,[57] with no correction for instrumental broadening, was performed on select peaks. The analysis indicated that the crystallite size (calculated from the subcell peaks) was 770 Å, whereas the ordered domain size (calculated from supercell peaks) was 380 Å. Higher resolution data collection and subtraction of the instrumental broadening function is necessary to obtain quantitatively accurate values, but the preliminary analysis clearly indicates the presence of antiphase boundaries in $NdAgTi_2O_6$.

Discussion

The formation of $Ca_2AgNdTi_4O_{12}$ as a single-phase perovskite, shows the potential of the POTATO/HPHT approach. The striking agreement between the predicted and observed bond valences for this compound demonstrates the ability of POTATO to accurately predict hypothetical perovskite structures. The formation of this compound together with $AgNdTi_2O_6$ clearly shows the HPHT route to be capable of incorporating the Ag^+ cation into the perovskite structure. This incorporation is not generally possible using conventional solid-state synthesis techniques.

The formation of multiple perovskite phases in the case of $Sr_2AgNdTi_4O_{12}$ could also be anticipated from the predictive modeling, which showed that the $b^-a^+b^-$ tilt system is incapable of simultaneously satisfying the valence requirements of Sr^{2+}, Ag^+, and Nd^{3+}. For this composition, the bond valences of the $a^0b^+b^+$ structure were more reasonable; however, it appears to have been naive to expect that the largest A-site cation, Ag^+, would occupy a square planar site in preference to the 8-coordinate A-site found in $b^-a^+b^-$ perovskites. The probability of Ag^+ occupying the square planar site was further diminished by the high-pressure synthesis, which favors the more efficient ion packing of the $b^-a^+b^-$ tilt system.

(56) Woodward, P. M.; Hoffmann, R. D.; Sleight, A. W. *J. Mater. Res* **1994**, *9*, 2118.
(57) Karen, P.; Woodward, P. M. submitted for publication in *J. Solid State Chem*.

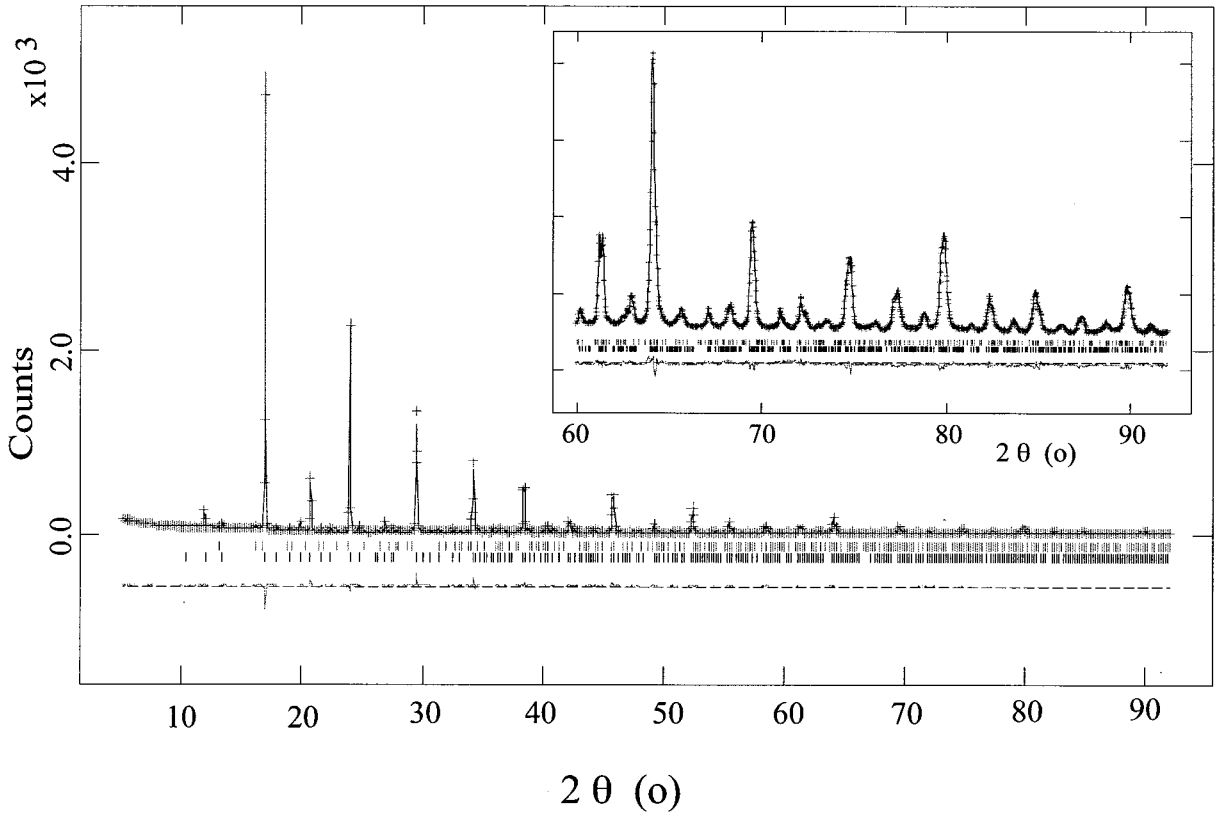

Figure 1. Results of Rietveld refinement of the structure of $Ca_2NdAgTi_4O_{12}$ at room temperature. The upper and lower ticks indicate the positions of reflections from the high-pressure TiO_2 phase and $Ca_2NdAgTi_4O_{12}$, respectively. The difference curve is shown in the bottom on the same scale. The high-angle area ($60° < 2\theta < 92°$) is magnified.

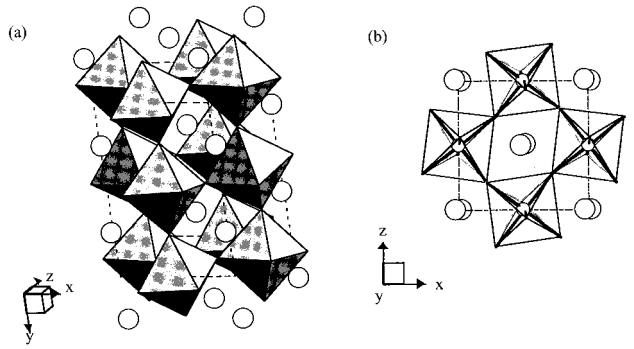

Figure 2. (a) TiO_6 octahedral linkages of $Ca_2NdAgTi_4O_{12}$. The unit cell is indicated by a dashed line. Open circles represent disordered Ca/Ag/Nd sites. (b) The projection of the structure on the *xz* plane. Ti are represented as smaller circles in the center of octahedra.

The failure of $Sr_2AgLaRu_4O_{12}$ to form a single-phase perovskite was completely unexpected from the modeling calculations. Apparently, even though a perovskite with this composition would be stable, the formation of such a compound from the starting materials is an endothermic process, illustrating an important limitation of the current approach. This problem might be overcome by incorporating thermodynamic calculations into the modeling process. To do this it is necessary to have available the equations of state (EOS) for the starting components, to evaluate ΔV for the breakdown reaction, and bond valence parameters valid at high temperatures and pressures. Although EOS are not currently available for many compounds at high pressures, such data are becoming increasingly available, and it might be possible to incorporate such calculations into the POTATO approach in the future.

The structure of $AgNdTi_2O_6$ is rather interesting. One way of visualizing the structure is to consider stacking of NdO^+, AgO^-, and TiO_2 layers in a Nd−Ti−Ag−Ti−⋯ sequence. The oxygen ions in the TiO_2 layers (O3) are shifted by 0.12 Å toward the NdO^+ layer, whereas the titanium ions are essentially equidistant from the NdO^+ and AgO^- layers. This distortion is driven by the electrostatic attraction of oxygen to the positively charged NdO^+ layer. It is interesting to compare this distortion with the one observed in $La_{0.55}Li_{0.33}\square_{0.12}TiO_3$, where lanthanum is both larger and more highly charged than lithium.[19] In that compound, the oxygen ions also have an electrostatic attraction to the positively charged lanthanum-rich layers, but ion−ion repulsion and/or the valency requirements of the smaller Li^+ cation cause the O3 ion to shift 0.03 Å toward the negatively charged lithium-rich layer. However, electrostatic interactions do result in a 0.14 Å shift of the Ti^{4+} ions toward the lithium-rich layer. This results in a very long (2.05−2.08 Å) distance between titanium and the oxygen in the lanthanum-rich layer, giving rise to one long and five short Ti−O bonds. Consequently, the octahedral distortions in $La_{0.55}Li_{0.33}\square_{0.12}TiO_3$ and $AgNdTi_2O_6$ are very different, but these distortions appear to be mainly driven by the size and charge of the A cations rather than Ti−O covalent bonding interactions.

$AgNdTi_2O_6$ represents the first example of A-cation ordering, driven by charge and/or size differences, in a compound with a single octahedral cation and a 1:1 A:A' ratio. Why is this type of ordering so rare and what attributes of $AgNdTi_2O_6$ are responsible for stabilizing the layered A-cation ordering? To answer these ques-

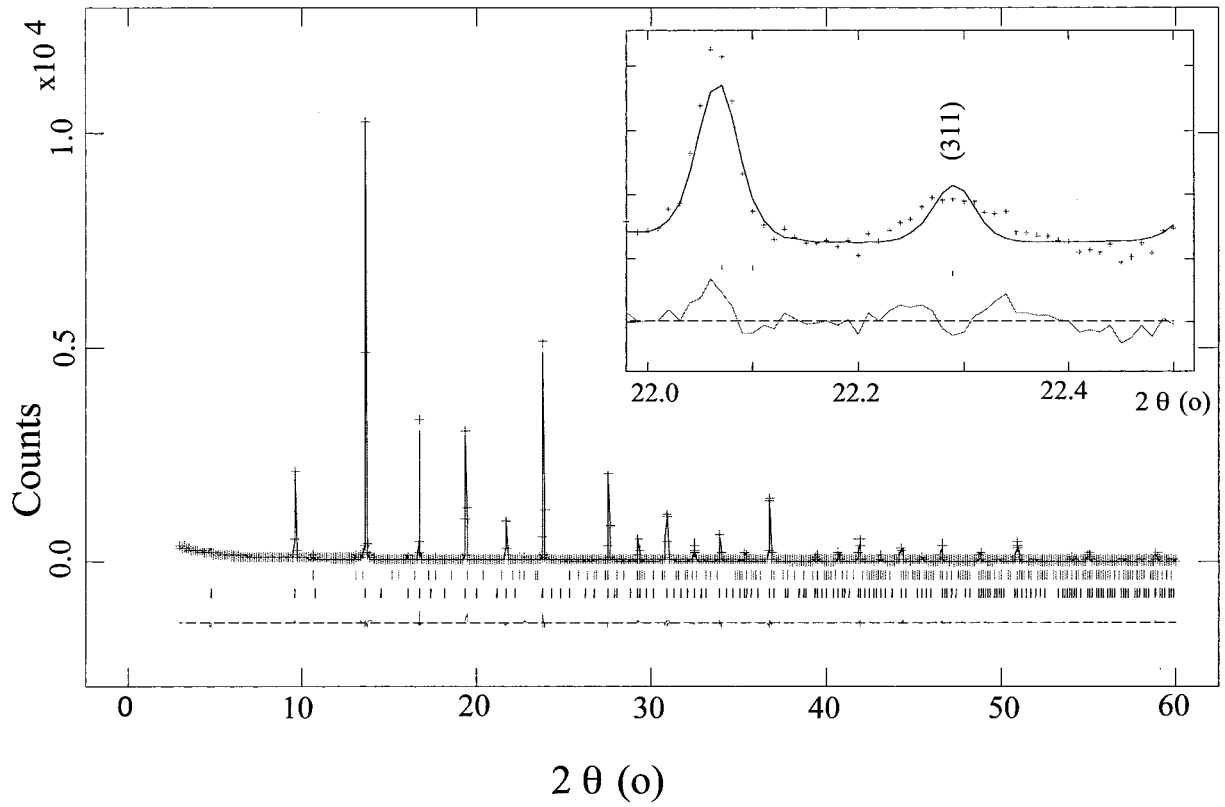

Figure 3. Results of Rietveld refinement of the structure of $NdAgTi_2O_6$ at room temperature. The upper and lower ticks indicate the positions of reflections from the high-pressure TiO_2 phase and $NdAgTi_2O_6$, respectively. The difference curve is shown in the bottom on the same scale. The angle region between 22° and 22.5° is magnified in the box above to show the superlattice peak such as (311). The peak broadness indicates partial ordering of Nd^{3+} and Ag^{1+} between the two available A cation sites.

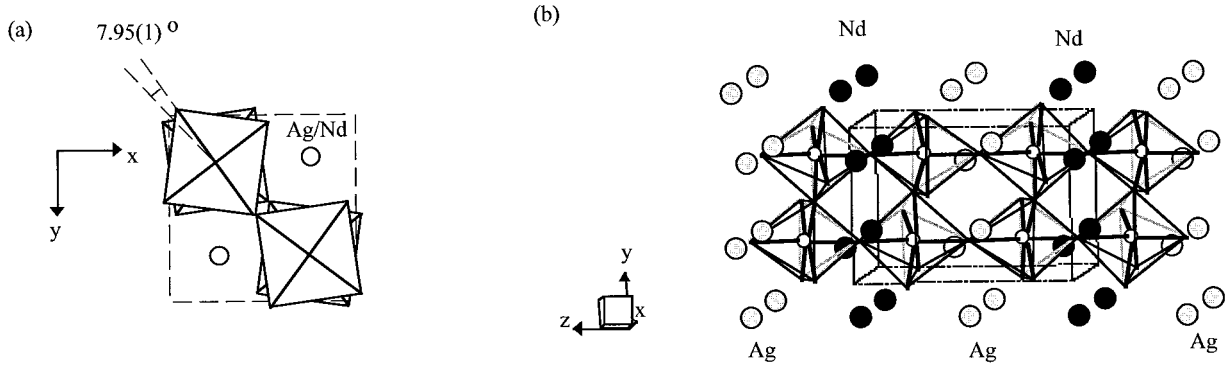

Figure 4. Projection of the structure of $NdAgTi_2O_6$ (a) on the *xy* plane showing the 7.95(1)° octahedral tilting angle along the *c* axis. (b) TiO_6 octahedral linkages of $NdAgTi_2O_6$ with O3 in the TiO layer shifted toward Nd^{3+}. The unit cell is indicated by a dashed line. Shaded and closed circles represent Ag and Nd dominated sites, respectively.

Table 7. Madelung Energy Calculations of Various Ordered Perovskites

compound	M^{3+}—O (Å)	M^{5+}—O (Å)	A^{+}—O (Å)	A^{3+}—O (Å)	Madelung energy per Ti (kJ/mol)	ordering energy (% change)
$A^{2+}M^{4+}O_3$[a]	—	—	—	—	−17 638	0
$A_2M^{3+}M^{5+}O_6$[b]	6 × 1.90	6 × 1.90	—	—	−17 949	1.8
$A_2M^{3+}M^{5+}O_6$[b]	6 × 2.03	6 × 1.87	—	—	−18 236	3.4
$A_2M^{3+}M^{5+}O_6$[b]	6 × 1.87	6 × 2.03	—	—	−17 689	0.3
$A^{+}A^{3+}M_2O_6$[c]	—	—	12 × 2.76	12 × 2.76	−17 776	0.8
$A^{+}A^{3+}M_2O_6$[c]	—	—	4 × 2.76	4 × 2.76	−17 469	−1.0
			8 × 2.68	8 × 2.84		
$A^{+}A^{3+}M_2O_6$[c]	—	—	4 × 2.76	4 × 2.76	−17 936	1.7
			8 × 2.84	8 × 2.68		

[a] Ideal perovskite structure, a = 3.90 Å, space group $Pm3m$. [b] Ordered cubic perovskite structure, a = 7.8 Å, space group $Fm3m$. [c] Layered A-cation ordered structure, a = 3.9 Å, c = 7.8 Å, space group $P4/mmm$.

tions, a series of Madelung energy calculations were carried out on idealized structures. The results are listed in Table 7. First, the Madelung energy of a cubic $A^{2+}M^{4+}O_3$ structure, with A−O and M−O distances of 2.76 and 1.90 Å, respectively, was calculated. Then, without altering bond distances, the cation distribution

was changed to simulate rock salt ordering of M^{3+}/M^{5+} and layered ordering of A^{+}/A^{3+}. Although both types of ordering are energetically favored, the stabilization energy associated with M^{3+}/M^{5+} ordering is more than twice as large as the stabilization accompanying A^{+}/A^{3+} ordering. This result helps to explain why M-cation ordering is so much more prevalent than A-cation ordering.[58] Each ordered structure can be further stabilized with respect to the disordered structure by shifting the oxygen ions closer to the higher valent cation (either M^{5+} or A^{3+}). Thus, the size difference between Ag^{+} (1.28 Å) and Nd^{3+} (1.11 Å), which results in a shift of the oxygen ions toward the higher valent neodymium cation, plays an important role in stabilizing the ordered structure. By comparison, the size difference between Na^{+} (1.18 Å) and La^{3+} (1.16 Å) is much smaller, and therefore, it is not surprising that ordering is not observed in $NaLaTi_2O_6$.[25]

Conclusions

Two highly crystalline perovskites containing Ag^{+}, $Ca_2AgNdTi_4O_{12}$, and $NdAgTi_2O_6$, have been synthesized using HPHT methods. The realization of a high-temperature synthetic route that allows the incorporation of Ag^{+} into the perovskite lattice should open the door to synthesis of a wide range of new perovskites. A rare example of layered A-cation ordering was observed in $NdAgTi_2O_6$. Calculations show that this type of ordering is not as energetically favorable as rock salt ordering of the octahedral cations. In fact, despite the charge difference and large size difference between Ag^{+} and Nd^{3+}, only partial ordering was achieved.

The utility of POTATO as a predictive tool for synthesis of new perovskites was demonstrated. In two of three cases, the modeling predictions were consistent with the synthesis results. The failed synthesis of $Sr_2AgLaRu_4O_{12}$ illustrates a potential pitfall of this approach; that is, even though POTATO modeling may produce a reasonable structure, the formation of this structure may not be thermodynamically favored. Consideration of the energies of competing phases may help to correct this problem. The goal of synthesizing a perovskite with the $a^0b^+b^+$ tilt system was not realized, apparently because the large size of the Ag^{+} cation and the more efficient packing density of the $b^-a^+b^-$ tilt system favor the latter tilt system over the former.

The modeling efforts described in this paper were carried out at a very rudimentary level. Cation shifts were neglected and bond valences were only roughly optimized. The incorporation of bond valence sums and least squares minimization algorithms into the POTATO program would greatly enhance its predictive ability and ease of use. Consideration of competing structures would also enhance the predictive ability of POTATO. Such efforts are currently underway. We feel that once such improvements have been made, POTATO will be a powerful tool that, in combination with other empirical and theoretical insights, can help to overcome the limitations inherent in the high-pressure synthesis of new materials.

Acknowledgment. J.-H. Park and J.B. Parise appreciate the financial support of the NSF (DMR-9713375/EAR-8920239). This work was also partially supported by the Division of Materials Sciences, U.S. Department of Energy, under contract No. DE-AC02-98CH10886. The NSLS is supported by the U.S. Department of Energy, Division of Materials Sciences and Division of Chemical Sciences.

CM980212J

(58) The charge difference between ions also plays an important role. For rock salt ordering of M/M' cations, an ordered arrangement is sometimes observed when the charge difference is two and almost always observed when the charge difference equals or exceeds four. However, the choice of oxidation states among available A-site cations normally limits the charge difference on the A-site to either two or three.